HAL
open science

# Effective targeting of STAT5-mediated survival in myeloproliferative neoplasms using ABT-737 combined with rapamycin

G Li, K Miskimen, Z. Wang, Xiu Yan Xie, W Tse, F. Gouilleux, R Moriggl, K Bunting

## To cite this version:

G Li, K Miskimen, Z. Wang, Xiu Yan Xie, W Tse, et al.. Effective targeting of STAT5-mediated survival in myeloproliferative neoplasms using ABT-737 combined with rapamycin. Leukemia, 2010, 24 (8), pp.1397-1405. 10.1038/leu.2010.131 . hal-02424599

**HAL Id: hal-02424599**

**https://univ-tours.hal.science/hal-02424599v1**

Submitted on 29 Oct 2021

**HAL** is a multi-disciplinary open access archive for the deposit and dissemination of scientific research documents, whether they are published or not. The documents may come from teaching and research institutions in France or abroad, or from public or private research centers.

L'archive ouverte pluridisciplinaire **HAL**, est destinée au dépôt et à la diffusion de documents scientifiques de niveau recherche, publiés ou non, émanant des établissements d'enseignement et de recherche français ou étrangers, des laboratoires publics ou privés.

NIH Public Access

## Manuscript Information

**Journal name:** Leukemia : official journal of the Leukemia Society of America, Leukemia Research Fund, U.K

**NIHMSID:** NIHMS202705

**Manuscript Title:** Effective targeting of STAT5-mediated survival in myeloproliferative neoplasms using ABT-737 combined with rapamycin

**Principal Investigator:**

**Submitter:** Nature Publishing Group (repositorynotifs@nature.com)

## Grant/Project/Contract/Support Information

| Name | Support ID# | Title |
|---|---|---|

## Manuscript Files

| Type | Fig/Table # | Filename | Size | Uploaded |
|---|---|---|---|---|
| manuscript | 1 | article_1.doc | 300544 | 2010-05-07 03:05:33 |
| figure | 1 | figure_1.tif | 779374 | 2010-05-07 03:05:34 |
| figure | 2 | figure_2.tif | 13775966 | 2010-05-07 03:05:49 |
| figure | 3 | figure_3.tif | 494166 | 2010-05-07 03:05:50 |
| figure | 4 | figure_4.tif | 643630 | 2010-05-07 03:05:51 |
| figure | 5 | figure_5.tif | 1607628 | 2010-05-07 03:05:52 |
| figure | 6 | figure_6.tif | 843410 | 2010-05-07 03:05:53 |
| figure | 7 | figure_7.tif | 592176 | 2010-05-07 03:05:54 |
| supplement | 1 | supp_info_1.doc | 63488 | 2010-05-07 03:05:54 |
| supplement | 2 | supp_info_2.tif | 499186 | 2010-05-07 03:05:55 |
| supplement | 3 | supp_info_3.tif | 437350 | 2010-05-07 03:05:55 |
| supplement | 4 | supp_info_4.tif | 1711428 | 2010-05-07 03:05:57 |
| supplement | 5 | supp_info_5.tif | 4533138 | 2010-05-07 03:06:01 |

This PDF receipt will only be used as the basis for generating PubMed Central (PMC) documents. PMC documents will be made available for review after conversion (approx. 2-3 weeks time). Any corrections that need to be made will be done at that time. No materials will be released to PMC without the approval of an author. Only the PMC documents will appear on PubMed Central -- this PDF Receipt will not appear on PubMed Central.

# Effective targeting of STAT5-mediated survival in myeloproliferative neoplasms using ABT-737 combined with rapamycin

Geqiang Li[1], Kristy L. Miskimen[1], Zhengqi Wang[1,7], Xiu Yan Xie[2], William Tse[1,5,6], Fabrice Gouilleux[3], Richard Moriggl[4], and Kevin D. Bunting[1,6,7]

[1]Department of Medicine, Division of Hematology-Oncology, Case Western Reserve University, Cleveland, OH
[2]Department of Pathology, Summa Health Barberton Hospital, Barberton, OH
[3]Department of Medicine, Immunology, INSERM, Amiens
[4]Ludwig Boltzmann Institute for Cancer Research, Vienna, Austria
[5]Current address: Department of Medicine, West Virginia University, Mary Babb Randolph Cancer Center, Morgantown, WV
[6]Case Comprehensive Cancer Center, Cleveland, OH
[7]Current address: Department of Pediatrics, Aflac Cancer Center and Blood Disorders Service, Emory University, Atlanta, GA

Running title: Targeting STAT5 survival signals

Correspondence:
Kevin D. Bunting, Ph.D.
Department of Pediatrics
Aflac Cancer Center and Blood Disorders Service
Emory University School of Medicine
2015 Uppergate Dr. NE, ECC #444
Atlanta, GA 30322
Tel: 404-778-4039
Fax: 404-727-4455
Email: kevin.bunting@emory.edu

Keywords: cytokine signaling, JAK/STAT, hematopoiesis, leukemogenesis, flow cytometry, hematopoietic stem cell

Abstract word count: 195
Manuscript pages: 21
Number of figures: 7
Number of supplemental figures: 4
Number of references: 39

This work was supported by NIH R01DK059380 (K.D.B), The Center for Stem Cell and Regenerative Medicine, SFB-F28 (R.M.) and the Flow Cytometry, Radiation Resources, and Histology Core Facilities of the Case Comprehensive Cancer Center (P30CA43703).

**Abstract:**

Signal transducer and activator of transcription-5 (STAT5) is a critical transcription factor for normal hematopoiesis and its sustained activation is associated with hematologic malignancy. A persistently active mutant of STAT5 (STAT5a$^{S711F}$) associates with Grb2 associated binding protein 2 (Gab2) in myeloid leukemias and promotes growth *in vitro* through AKT activation. Here we have retrovirally transduced wild-type or Gab2$^{-/-}$ mouse bone marrow cells expressing STAT5a$^{S711F}$ and transplanted into irradiated recipient mice to test an *in vivo* myeloproliferative disease (MPD) model. To target Gab2-independent AKT/mTOR activation, wild-type mice were treated separately with rapamycin. In either case, mice lacking Gab2 or treated with rapamycin displayed attenuated myeloid hyperplasia and modestly improved survival, but the effects were not cytotoxic and were reversible. To improve upon this approach, *in vitro* targeting of STAT5-mediated AKT/mTOR using rapamycin was combined with inhibition of the STAT5 direct target genes bcl-2 and bcl-$X_L$ using ABT-737. Striking synergy with both drugs was observed in mouse BaF3 cells expressing STAT5a$^{S711F}$, TEL-JAK2, or BCR-ABL and in the relatively single agent-resistant human BCR-ABL positive K562 cell line. Therefore, targeting distinct STAT5 mediated survival signals, e.g. bcl-2/bcl-$X_L$ and AKT/mTOR may be an effective therapeutic approach for human myeloproliferative neoplasms.

**Introduction:**

Signal transducer and activator of transcription-5 (STAT5) is a latent transcription factor that can be activated by phosphorylation by Janus kinases (JAKs) in the cytoplasm, leading to dimerization, DNA binding, and retention within the nucleus(1). Tyrosine phosphorylated STAT5 can be tracked by flow cytometry or immunostaining and is a biomarker associated with poor prognosis for juvenile myelomonocytic leukemia(2) and acute myeloid leukemia(3). Recently, targeting transcription factor – cofactor complexes has become clinically plausible(4, 5). However, targeting of pSTAT5 or its aberrant signaling might be difficult and risky since complete inhibition of STAT5 may present significant side effects, e.g. in

hematopoietic cell types and liver function. Therefore, understanding aberrant STAT5 signaling in normal vs. leukemic cells may allow for novel strategies for leukemia therapy.

Cooperative interactions and downstream targets of STAT5 responsible for its function in hematopoiesis are not well defined. Constitutive STAT5 activation with double mutant STAT5a$^{H299R,S711F}$ causes myeloproliferative disease (MPD) in mice(6) and this disease development requires STAT5 expression in the hematopoietic stem cell (HSC)(7). In studies using the single mutant STAT5a$^{S711F}$, myeloid and lymphoid hyperplasias have been described(8, 9). To date most functions for STAT5 have been attributed to a growing list of well characterized direct target gene products such as *Osm*, *Cis*, *Socs*, *Pim1*, *Bcl-X$_L$* and *c-Myc*. We have recently shown that expression of bcl-2/bcl-X$_L$ mediated by STAT5 requires the N-domain and is critical for lethal MPD in mice(10).

STAT5 and phosphatidylinositol-3'-kinase (PI3-K) activation are required for pro-survival signaling(11) and cross-talk between these pathways has been described downstream of interleukin (IL)-2(12) and thrombopoietin (TPO)(13) receptors. Enhanced sensitivity to inhibition of STAT5, SHP-2, and Grb2-associated binding protein (Gab2)(14) was found in Bcr/Abl transformed cell lines. Cytoplasmic localization of phosphorylated STAT5 has recently been described, whereby STAT5 interacts with Gab2(8, 15) or with Shc, which in turn interacts with Grb2 and Gab2(16). In each case phosphorylated STAT5 promoted activation of Akt suggesting that Gab2/Akt might be a potential therapeutically relevant signaling node in hematologic malignancies. Gab2 is tyrosine phosphorylated by several early acting cytokine receptors such as Flt3, c-Kit, IL-3R, and c-Mpl and contains binding sites for SH2 and SH3 domains that promote binding to signaling molecules(17-19). Gab2 is involved in promoting the activation of the PI3-K and the mitogen activated protein kinase (MAPK) pathways and can regulate hematopoietic cell survival and migration functions(20). In BaF3 cells, Gab2 was found to associate indirectly with persistently active STAT5, p85, and Grb2, but not SHP-2 and to promote STAT5-mediated signaling through induction of

PI3-K and MAPK pathways(8, 15, 21, 22). This interaction required phosphorylation of STAT5. The STAT5-Gab2 complex was also observed in primary cells obtained from mice expressing STAT5a$^{S711F}$ where increased Akt activation was observed (8).

In the studies reported here, we directly asked whether STAT5/Gab2 contribute to leukemic hematopoiesis *in vivo* by testing the genetic impact of Gab2 deficiency. We also tested the therapeutic efficacy of targeting the PI3K/Akt/mTOR pathway pharmacologically in STAT5-provoked MPD using rapamycin. The results indicated that this pathway can modulate cell growth but that targeting multiple STAT5-mediated survival signals including bcl-2/bcl-$X_L$ is required for efficient killing of myeloproliferative neoplasm cells.

**Materials and Methods:**

***Cell lines, plasmids, and antibodies –*** Murine stem cell virus (MSCV) vectors expressing green fluorescent protein (GFP) from an internal ribosomal entry sequence (IRES; IR) were generated for MSCV-STAT5a-IR-GFP and MSCV-STAT5a$^{S711F}$-IR-GFP as described previously(9). All GP+E86 based retroviral producer cell lines were cultured in Hyclone Dulbecco's Modified Eagles Medium (DMEM) containing 10% Calf serum (Hyclone), 1% penicillin, 1% streptomycin and 1% amphotericin B (complete medium) at 37°C in an atmosphere of 95% oxygen and 5% $CO_2$. BaF3 and NB4 cells were maintained in RPMI 1640 medium and K562 were maintained in Iscove's Modified Dulbecco's Medium (IMDM). All antibodies are described in Supplemental Methods.

***Mice –*** The C57BL/6 (CD45.2) mice and the congenic B6.SJL-Ptprc$^{a}$Pep3$^{b}$/BoyJ (CD45.1) strain were obtained from the Jackson Laboratory (Bar Harbor, ME). All mutant mice were on the C57BL/6 background and housed in a specific pathogen-free environment. All mouse studies were approved by the Institutional Animal Care and Use Committee at Case Western Reserve University.

***Retroviral vector transduction and transplantation*** – Retroviral transduction of wild-type or Gab2$^{-/-}$ BM was performed using concentrated retroviral supernatant and colony-forming unit in culture (CFU-C) assays were performed as described(23, 24). Five independent transduction experiments were performed with 0.8 to 4 million transduced BM cells transplanted per recipient mouse as described in *Results*. Typical donor: recipient ratios for these experiments were from 1.5:1 to 2:1. All adult recipient mice were conditioned with 950 rads of irradiation from a $^{137}$Cs source 3 to 6 hours prior to cell injection.

***Histology and flow cytometry of mouse tissues*** -- Transplanted mice were euthanized when becoming moribund and the tissue specimens were prepared from freshly killed mice. Tissues were fixed in 10% neutral buffered formalin and embedded in paraffin. Paraffin sections (4 μm) were stained with hematoxylin and eosin (H&E). Histological sections and stains were performed by the Case Comprehensive Cancer Center Histology core lab. Images were taken using an Olympus BX41 microscope equipped with PanAchromatic objectives (20X, 40X) and a mounted Spot In-Sight digital camera (Diagnostic Instrument Inc.). The software for image acquisition was Spot Advance™. Cells from live mice were analyzed by flow cytometry as described in *Supplemental materials*.

***Drug treatments*** -- Rapamycin (LC Laboratories) was initially dissolved in 100% ethanol, stored at –20°C, and further diluted in an aqueous solution of 5.2% Tween and 5.2% polyethylene glycol 400 (2% final ethanol concentration) immediately before use. Transplanted mice were treated with rapamycin (4 mg per kg i.p.) every other day for 3-4 weeks and then discontinued. ABT-737 (Abbott Laboratories) was dissolved in DMSO and stored in aliquots at -20$^{0}$C. BaF3 cells were cultured in the indicated concentration of rapamycin or ABT-737 and cell proliferation/viability was determined by either propidium iodide staining or trypan blue exclusion assay. Both methods gave comparable percentages of cell death. Western blots were performed as previously described(21).

***Statistical analyses*** – To test for genetic interaction, two-way ANOVA analysis was used. We also used Wilcoxan-Mann-Whitney U tests for wild-type vs. mutant single comparisons. *P* values of less than 0.05 were considered statistically significant and were calculated using SPSS16.0 (SPSS, Inc.). Student's two-tailed T tests were performed using InStat 1.5 (University of Reading, UK). Kaplan-Meier comparisons were analyzed by log-rank test.

**Results:**

Since our prior studies have shown evidence for STAT5-mediated activation of the PI3K pathway, we set out in these studies to interrogate the impact of PI3K signaling on a STAT5-provoked MPD *in vivo*. This is important to assess as a potential therapeutic approach since persistent STAT5 activation is a hallmark of myeloid hyperproliferation and myeloid cytokines and growth factors also activate STAT5. Our studies utilized both genetic and pharmacologic modulation of the PI3K pathway to test the impact upon MPD induced by transplantation of BM cells expressing STAT5a$^{S711F}$ into recipient mice (**Fig. S1**).

We examined whether there was a difference in the retroviral transduction efficiency between the wild-type and Gab2$^{-/-}$ BM cells. Similar transduction efficiencies were observed in both groups prior to transplantation within each experiment as determined by the percentage of GFP$^{+}$ cells which ranged from 10-40% for IR-GFP and 10-30% for STAT5a$^{S711F}$ vector. Comparable levels of gene transfer (GFP$^{+}$ cells) *in vivo* were also observed for the IR-GFP marking vector control in either wild-type or Gab2$^{-/-}$ BM recipient mice (data not shown), thus indicating that Gab2 deficiency did not impair transduction of cells capable of repopulating hematopoiesis. No defect in homing of c-Kit$^{+}$ progenitors from wild-type or Gab2$^{-/-}$ BM cells was observed (data not shown) and mice engrafted with STAT5a$^{S711F}$ expressing donor BM cells showed marked expansion of the myeloid lineage but did not expand lymphoid or erythroid populations (data not shown).

**Gab2 deficiency attenuates MPD and improves survival associated with activated STAT5**

Since STAT5a$^{S711F}$ was incapable of conferring cytokine-independent growth to myeloid CFU-C, we tested the impact of Gab2 deficiency on murine MPL$^{W506L}$-induced cytokine independent CFU-C. Gab2 deficiency conferred a reduction in colony number (**Fig. S2**). To gain further insight into the contribution of Gab2 to STAT5a$^{S711F}$ induced MPD *in vivo*, BM cells from wild-type or Gab2$^{-/-}$ mice were transduced with the IR-GFP control vector or STAT5a$^{S711F}$ expressing vector. The cells were then transplanted into lethally irradiated recipient mice. The engrafted mice were analyzed 4-6 weeks after transplantation. As expected, flow cytometry analyses showed that all wild-type mice expressing STAT5a$^{S711F}$ had an increased frequency of Gr-1$^{+}$Mac-1$^{+}$ cells compared to the empty vector control in the peripheral blood. Regardless of the myeloid frequencies, the WBC counts from the mice transplanted with Gab2$^{-/-}$ background BM expressing STAT5a$^{S711F}$ were significantly lower than those receiving the wild-type counterpart (**Fig. 1A**; P=0.001; Mann-Whitney U test). The absolute number of Gr-1$^{+}$Mac-1$^{+}$ cells was accordingly reduced 3- to 4-fold relative to wild-type counterparts (**Fig. 1B**; P=0.014; Mann-Whitney U test). The genetic interaction between Gab2 and STAT5a$^{S711F}$ was advantageous for elevated WBC counts and myeloid cell expansion (WBC: P<0.001; 2-way ANOVA; Myeloid cells: P=0.022; 2-way ANOVA), indicating that STAT5a$^{S711F}$ can cooperate with Gab2 to induce myeloid hyperplasia.

At the time of death, tissues from mice were collected and analyzed to determine the degree of myeloid infiltration. Corresponding to the reduced peripheral myeloid expansion, spleen weights were reduced 2- to 3-fold for STAT5a$^{S711F}$ expressed in Gab2$^{-/-}$ background relative to STAT5a$^{S711F}$ expressed in wild-type background cells (**Fig. 1C**; P=0.001; Mann-Whitney U test). Genetic interaction between STAT5a$^{S711F}$ and Gab2 was observed (P<0.001; 2-way ANOVA), consistent with our previous report of biochemical interaction between STAT5a$^{S711F}$ and Gab2(8). No mice died following transplant with control IR-GFP expressing vector regardless of the genotype of the starting BM cells. The attenuated MPD

was sufficient to improve survival, although most recipients of Gab2$^{-/-}$ background BM cells eventually died from MPD 68 days post transplant (**Fig. 1D**).

Tissue histology of mice receiving wild-type or Gab2$^{-/-}$ background transduced BM cells was compared at the time of euthanasia. In the liver of wild-type mice expressing STAT5a$^{S711F}$, the hepatic lobular architecture was markedly distorted by dense infiltration of mostly mature myeloid cells but including rare early precursors in the hepatic lobules or portal triads (**Fig. 2A**). However, in the mice transplanted with Gab2$^{-/-}$ background BM cells, the hepatic architecture was largely intact with significantly less infiltrate in the hepatic lobules or periportal areas. In the spleen, the wild-type mice expressing STAT5a$^{S711F}$ showed pronounced splenomegaly (~5-fold) with markedly distorted splenic architecture (**Fig. 2B**). The red and white pulps were diffusely effaced by extramedullary hematopoiesis and myelomonocytic cells at mostly immature stages of differentiation. However, the splenic architecture for STAT5a$^{S711F}$ on the Gab2$^{-/-}$ background was largely intact and associated with ~2-fold elevated spleen weights. Spleen and liver of wild-type mice expressing STAT5a$^{S711F}$ showed increased percentages of Gr-1$^{+}$Mac-1$^{+}$ myeloid lineage cells. In contrast, there was markedly less myeloid involvement in spleen and liver of mice receiving Gab2$^{-/-}$ BM cells expressing STAT5a$^{S711F}$. In the absence of Gab2, about half of the mice expressing STAT5a$^{S711F}$ died early and had higher percentages of myeloid cells than those that survived longer (**Fig. S3A**). Notably, significant expansion of non-GFP$^{+}$ cells was also observed (**Fig. S3B**).

**Persistently active STAT5 induces Akt activation in myelomonocytic infiltrates**

Although Gab2 deficiency attenuated the MPD by STAT5a$^{S711F}$ *in vivo*, it didn't fully block the MPD progression. Previous reports indicated that STAT5a$^{S711F}$ can induce Akt activation *in vitro* and we showed that TAT-Gab2 decoy molecules can significantly block this Akt activation(8). We therefore next examined the pAkt level in the spleen of mice transplanted

with wild-type or Gab2$^{-/-}$ BM cells expressing either empty vector or STAT5a$^{S711F}$. A similar basal level of Akt activation was observed in the mice transplanted with IR-GFP vector expressing BM cells of either genotype (**Fig. S4A**). However, there was a dramatic increase in the number of positive cells for phosphorylated species of Akt staining in mice transplanted with wild-type or Gab2$^{-/-}$ BM cells expressing STAT5a$^{S711F}$ (**Fig. S4B**). The pAkt positive cells correlated with the expanding myeloid population in the tissues, consistent with the finding that more myeloid infiltration occurs in the liver of mice transplanted with wild-type BM cells expressing STAT5a$^{S711F}$.

**Rapamycin treatment is cytostatic and delays MPD induced by persistently active STAT5**

To determine whether targeting downstream of Gab2-mediated PI3K/Akt signaling would be effective, rapamycin was used to target mTOR. Rapamycin was very effective at reducing the number of CFU-C driven by either STAT5a$^{S711F}$ cultured in 2 ng/ml IL-3 **Fig. 3A**) or MPL$^{W506L}$ (**Fig. 3B**) in the absence of cytokines. In the presence of IL-3, IL-6, and SCF, a trend toward reduced CFU-C was observed but it was not significant (**Fig. 3B**). The observation that STAT5 hyperactivation induced Akt activation *in vivo* provided a potential therapeutic target. mTOR, a serine/threonine kinase downstream of Akt, is involved in regulation of the cell cycle, apoptosis, and angiogenesis. Tumors harboring dysregulated activation of the PI3K/Akt pathway are sensitive to mTOR inhibition(25). We next tested whether inhibition of mTOR activity could attenuate MPD promoted by STAT5a$^{S711F}$. Due to the rapid onset of MPD as early as 10 days after transplantation we decided to perform our drug treatments at the early stage of MPD. We delayed the disease by transplanting 0.8 to 1 million STAT5a$^{S711F}$ expressing BM cells into wild-type mice compared with 1.5 to 4 million for the Gab2$^{-/-}$ experiments. One month after transplantation when all mice were still healthy from appearance but had a significant fraction of GFP$^{+}$ cells in the peripheral blood, we injected rapamycin every other day (4 mg/kg,; i.p. injection or vehicle). The average % GFP$^{+}$ cells pre-treatment for all control (21 $\pm$ 10%; N=12) or rapamcyin (17 $\pm$ 5%; N=13) groups

was not significantly different (P=0.21, T-test). The average WBC counts pre-treatment for all control ($9.2 \times 10^6 \pm 7.9 \times 10^6$/ml; N=12) or rapamycin ($7.8 \times 10^6 \pm 4.0 \times 10^6$/ml; N=13) groups were not significantly different (P=0.58, T-test). Rapamycin treatment for 3-4 weeks followed by discontinued treatment resulted in a slight drop in WBC counts compared to vehicle treatment and relative to mice transplanted with BM cells transduced with the IR-GFP control retroviral vector (**Fig. 4A, 4B**). In contrast, mice transplanted with BM cells expressing STAT5a$^{S711F}$, showed a significant reduction in WBC count in a time span of 10 days after initiation of rapamycin treatment (Mann-Whitney U-test, P=0.002) (**Fig. 4C, 4D**). Control vehicle treatment had no effect on STAT5a$^{S711F}$ mediated MPD progression. Consistent with inhibition of STAT5a$^{S711F}$ induced myeloid outgrowth, the mice expressing STAT5a$^{S711F}$ had improved survival during the 3 weeks of treatment of rapamycin and lived approximately 1 month longer than the vehicle treated control group (**Fig. 4E**; P=0.03). All control mice died within two months of transplantation. Overall, rapamycin therapy reduced the outgrowth of the myeloid expansion by STAT5a$^{S711F}$ and attenuated progression of disease.

**Rapamycin synergizes with ABT-737 to inhibit cytokine-independent myeloid cell survival**

We next tested whether the mTOR inhibitor rapamycin would be effective at suppressing growth of a broader set of hematopoietic cells expressing human disease relevant mutations. BaF3 cells expressing STAT5a$^{S711F}$ were compared with BaF3 cells expressing BCR-ABL or TEL-JAK2. All 3 lines were cytokine-independent and all were sensitive to rapamycin-induced growth suppression. Cell lines expressing only the IR-GFP empty vector still required IL-3 for growth stimulation. The BaF3 cells were cultured in a low dose of 0.01 ng/ml IL-3 and this concentration was sufficient to keep the control cells alive during 48 hours without significant loss of viability. Overexpression of STAT5a$^{S711F}$ enhanced Akt activation and downstream phosphorylation of p70S6 kinase (p70S6K) and AKT relative to the IR-GFP control (**Fig. 5A**). Treatment with rapamycin for 24 hours at the concentration of

1 nM effectively blocked STAT5a$^{S711F}$ mediated growth and suppressed p70S6K without having any direct impact on STAT5 tyrosine or Akt serine phosphorylation. It is worthy to note that although rapamycin significantly inhibited proliferation (**Fig. 5B**), it didn't induce significant loss of cell viability in any of the BaF3 cell lines.

Since rapamycin alone was not effective at killing the BaF3 cells, rapamycin was combined with ABT-737, an inhibitor of bcl-2/bcl-$X_L$. ABT-737 was toxic in a dose-dependent manner up to 10 μM to all BaF3 cell lines (**Fig. 5C**). However, when 5 μM ABT-737 was combined with a concentration of 1 nM rapamycin, a striking synergy was observed in cell lines expressing TEL-JAK2, BCR-ABL, and STAT5a$^{S711F}$ increasing from ~20% to >80% killing (**Fig. 5D**). To extend this observation further, the effects of rapamycin or ABT-737 alone were assayed in human BCR-ABL positive K562 cells. Human myeloproliferative neoplasms are more complex genetically than the primary BM cell or BaF3 model cells. Despite inhibition of phosphorylation of p70S6K at concentrations above 10 nM (**Fig. 6A**), rapamycin alone had minimal effects on these cells (**Fig. 6B**). K562 cells were then exposed to ABT-737 which displayed very low toxicity at concentrations $\leq$ 5 μM and up to 30% death at 10 μM (**Fig. 6C**). However, the combination of 10 μM ABT-737 and a non-toxic concentration of 1 nM rapamycin gave a synergistic increase in the percentage of cell killing (**Fig. 6D**). In contrast, NB4 cells were more sensitive to rapamycin alone but showed no synergy when combined with ABT-737 (**Fig. 6E-H**) indicating that the effect is not generalizable to all types of leukemia cells. Various doses and timing were tested for NB4 cells and no evidence of synergy was observed (data not shown). Similar results were also obtained in HL-60 cells (data not shown).

**Discussion:**

Activation of STAT5 has been frequently observed in human myeloid leukemias and myeloproliferative disorders. Persistent activation of STAT5 in a mouse model mimics the

effect of upstream activating tyrosine kinases which tyrosine phosphorylate STAT5 to promote mouse MPD (**Fig. 7**). Our transplant model thus has relevance for leukemia and MPDs in patients. Important roles for STAT5 were reported in the propagation of BCR-ABL(26), Flt3-ITD(27), and TEL-PDGFR(28) induced leukemias in mouse models. The advantage of this model for study of downstream signaling from STAT5 is that the aberrant signaling is initiated by STAT5 and not through receptors that are capable of activating multiple different signaling pathways.

We have recently shown that persistently active STAT5a can interact physically with Gab2 to promote Akt activation in BaF3 cells and in primary BM cultures(8). However, the *in vitro* effects of TAT-Gab proteins on cell growth may not have recapitulated the complex intrinsic and extrinsic disease *in vivo*. Therefore, it was necessary to test the impact of PI3K pathway activation in oncogenic STAT5a-mediated MPD to establish the definitive role in a disease model. Although Gab2 was not essential for STAT5-induced leukemic expansion *in vivo*, Gab2 did play an important supportive role in several aspects of MPD induced by STAT5a$^{S711F}$. In the absence of Gab2, myeloid cells were reduced in peripheral blood and tissues like the liver, spleen weights were normalized, and overall survival was improved. These effects were also not related to transduction efficiency of the Gab2$^{-/-}$ host since levels of GFP$^{+}$ cells in the BM prior to transplant were comparable. Moreover, we have previously reported that the numbers of HSC and early progenitors are normal in the absence of Gab2(24). Additionally, the percentage of GFP$^{+}$ cells obtained using IR-GFP control were the same regardless of Gab2 genotype and we found that homing of Gab2$^{-/-}$ BM c-Kit$^{+}$ cells was normal.

Unlike prior studies we did not observe evidence of lymphoid hyperplasia induced by STAT5a$^{S711F}$. This is perhaps related to a very different transplant protocol which differs in 5-fluorouracil treatment that increased retroviral transduction efficiency (percentage of GFP$^{+}$ cells) and the use of pure C57BL/6 mouse strains for donor/host in these experiments

compared with prior studies that used C57BL/6 x 129/Sv F1 mice (which achieved ~5% $GFP^+$ cells(8, 9)). Overall, we did not observe expansion of a myeloblastic c-$Kit^+$ population in the transplant protocol. Thus, we refer to the disease as MPD instead of a myeloid leukemia. Of note, we observed expansion of non-transduced donor BM cells (GFP negative), indicating that STAT5-induced MPD may also involve cell extrinsic promoting factors. Oncostatin M is a myeloid cytokine and target gene of STAT5 which might partially explain this response. Similar cell extrinsic effects have been observed in retroviral models expressing TEL-JAK2(6) or $JAK2^{V617F}$ vectors(29) which activate both STAT5 proteins.

The presence of substantial phosphorylated Akt in the absence of Gab2 could be due to a number of possible alternative activation routes and will be the focus of future studies. Activation of cytokine receptor signaling through secreted growth factors such as IL-3 or GM-CSF is possible. Other Gab family members such as Gab1 or Gab3 could compensate for Gab2 in this disease model. All three Gabs are highly homologous and may play a redundant role in multiple aspects of hematopoietic development. Alternatively, STAT5 activation in the absence of Gab2 protein could lead to genetic compensation. Nevertheless, the phosphorylated Akt represented a key protein downstream of $STAT5a^{S711F}$/Gab2/PI3K and this led us to question whether efficient targeting by the inhibitor of mTOR would be effective in this model.

We utilized rapamycin to test whether it would have a similar efficacy in the $STAT5a^{S711F}$ MPD model as was observed in the $Gab2^{-/-}$ genetic background. Strikingly, treatment with rapamycin at the early stage of MPD was very effective at preventing further development and expansion of myeloid cells. This effect was cytostatic but did not prevent the subsequent recurrence of MPD once the treatment was stopped. Compared with the permanent deletion of Gab2, rapamycin treatment gave a similar response in regard to Gr-$1^+$/Mac-$1^+$ cell expansion and prolonged survival. Treatment with rapamycin in the transplant model is a very stringent system, since it was necessary to wait 4 weeks until

hematopoietic reconstitution before initiation of therapy, in order to prevent graft failure. To slow down disease progression, we injected fewer donor cells which allowed for a balance between donor engraftment and early disease development. In either the Gab2 genetic model or the rapamycin pharmacologic model, the survival was improved. Preliminary data shows that the combination of rapamycin and Gab2 targeting may be effective but this finding needs to be further tested *in vivo* and will be more challenging to translate to the clinic. While there is a complex interplay between Akt and the mTOR complexes and a negative feedback loop mediated by p70S6K inhibition of IRS controls serine 473 phosphorylation of Akt(30), we did not observe increased p70S6K in our BaF3 studies with our short 24h rapamycin treatment. However, with this in mind we may not have achieved the maximal attenuation of mTOR signaling *in vivo*, which may have limited our efficacy in controlling myeloid expansion and survival.

Rapamycin is an effective inhibitor of mTORC1 and has been previously shown to synergize with protein tyrosine kinase inhibitors (31, 32). Rapamycin also targets mcl-1 in glucocorticoid-resistant ALL (33) and the BH3 mimetic and bcl-2/bcl-$X_L$ inhibitor ABT-737 combined with various agents is synergistic due to effects on disabling resistance to the intrinsic apoptotic pathway. For example, in lung tumor xenografts, ABT-737 synergized with rapamycin (34) and the homolog ABT-263 synergized with rapamycin on lymphoma cells (35). We recently reported that induced expression of bcl-2 by STAT5 is critical for the development of lethal MPD (10). Therefore, we hypothesized that additional STAT5 direct target genes promoting cell survival might also need to be targeted. Indeed, we observed striking synergy in killing cells expressing BCR-ABL, TEL-JAK2, or mutant STAT5 when rapamycin was combined with ABT-737. Importantly, in the ABT-263 resistant cell line K562(36), which we show is relatively resistant to rapamycin and ABT-737 alone, was much more sensitive to the combination of rapamycin and ABT-737. In contrast, the classic APL subtype cell line NB4 that lacks constitutive STAT5 activation was not synergistically sensitive to the combined treatment. It is possible that STAT5 regulates mcl-1 or bcl-2A1

expression through both direct and indirect mechanisms to promote cell survival in MPD, comparable to recent demonstrations (37, 38). However, in this study we focused on the therapeutic end points and did not profile expression of all bcl-2 family members. Further analysis of additional STAT5 target genes may be important for optimization of the approach outlined in Fig. 7.

Overall, the similarity in response suggests that the in vivo STAT5a$^{S711F}$ model may be a useful tool for further testing drug combinations *in vivo* for their impact upon MPD progression and lethality. Targeting using specific Akt and PI3-K inhibitors or combination mTORC1/2 inhibitors (39) in our model may show even greater translational potential. Overall, our studies validate that the Gab2/PI3K/Akt/mTOR signaling axis is a therapeutic target capable of attenuating hematologic disease provoked by persistently active STAT5, which may find clinical use as an adjuvant in combination with drugs directed toward STAT5 target genes such as bcl-2 and bcl-$X_L$.

**Acknowledgments:**

We thank Henry Koon for critical review of the manuscript and Fang Xu for biostatistical support. We also thank Jalpa Patel and Emma Arriola at Abbott Laboratories for supplying ABT-737.

**Conflicts of Interest and Dual Publication Statements:**

The material is original research, has not been previously published and has not been submitted for publication elsewhere while under consideration. The authors also have no conflicts of interest to declare regarding the studies performed.

**References**

(1) Iyer J, Reich NC. Constitutive nuclear import of latent and activated STAT5a by its coiled coil domain. FASEB J. 2008; **22**: 391-400

(2) Kotecha N, Flores NJ, Irish JM, Simonds EF, Sakai DS, Archambeault S, az-Flores E, Coram M, Shannon KM, Nolan GP, Loh ML. Single-cell profiling identifies aberrant STAT5 activation in myeloid malignancies with specific clinical and biologic correlates. Cancer Cell 2008; **14**: 335-343

(3) Heuser M, Sly LM, Argiropoulos B, Kuchenbauer F, Lai C, Weng A, Leung M, Lin G, Brookes C, Fung S, Valk PJ, Delwel R, Lowenberg B, Krystal G, Humphries RK. Modelling the functional heterogeneity of leukemia stem cells: role of STAT5 in leukemia stem cell self-renewal. Blood 2009; **114**: 3983-3993

(4) Moellering RE, Cornejo M, Davis TN, Del BC, Aster JC, Blacklow SC, Kung AL, Gilliland DG, Verdine GL, Bradner JE. Direct inhibition of the NOTCH transcription factor complex. Nature 2009; **462**: 182-188

(5) Gorczynski MJ, Grembecka J, Zhou Y, Kong Y, Roudaia L, Douvas MG, Newman M, Bielnicka I, Baber G, Corpora T, Shi J, Sridharan M, Lilien R, Donald BR, Speck NA, Brown ML, Bushweller JH. Allosteric inhibition of the protein-protein interaction between the leukemia-associated proteins Runx1 and CBFbeta. Chem.Biol. 2007; **14**: 1186-1197

(6) Schwaller J, Parganas E, Wang D, Cain D, Aster JC, Williams IR, Lee CK, Gerthner R, Kitamura T, Frantsve J, Anastasiadou E, Loh ML, Levy DE, Ihle JN, Gilliland DG. Stat5 is essential for the myelo- and lymphoproliferative disease induced by TEL/JAK2. Mol Cell 2000; **6**: 693-704

(7) Kato Y, Iwama A, Tadokoro Y, Shimoda K, Minoguchi M, Akira S, Tanaka M, Miyajima A, Kitamura T, Nakauchi H. Selective activation of STAT5 unveils its role in stem cell self-renewal in normal and leukemic hematopoiesis. J.Exp.Med. 2005; **202**: 169-179

(8) Harir N, Pecquet C, Kerenyi M, Sonneck K, Kovacic B, Nyga R, Brevet M, Dhennin I, Gouilleux-Gruart V, Beug H, Valent P, Lassoued K, Moriggl R, Gouilleux F. Constitutive activation of Stat5 promotes its cytoplasmic localization and association with PI 3-kinase in myeloid leukemias. Blood 2007; **109**: 1678-1686

(9) Moriggl R, Sexl V, Kenner L, Duntsch C, Stangl K, Gingras S, Hoffmeyer A, Bauer A, Piekorz R, Wang D, Bunting KD, Wagner EF, Sonneck K, Valent P, Ihle JN, Beug H. Stat5 tetramer formation is associated with leukemogenesis. Cancer Cell 2005; **7**: 87-99

(10) Li G, Miskimen KL, Wang Z, Xie XY, Brenzovich J, Ryan JJ, Tse W, Moriggl R, Bunting KD. STAT5 requires the N-domain for suppression of miR15/16, induction of bcl-2, and survival signaling in myeloproliferative disease. Blood 2009; **115**: 1416-1424

(11) Um M, Lodish HF. Antiapoptotic effects of erythropoietin in differentiated neuroblastoma SH-SY5Y cells require activation of both the STAT5 and AKT signaling pathways. J.Biol.Chem. 2006; **281**: 5648-5656

(12) Moon JJ, Rubio ED, Martino A, Krumm A, Nelson BH. A permissive role for phosphatidylinositol 3-kinase in the Stat5-mediated expression of cyclin D2 by the interleukin-2 receptor. J.Biol.Chem. 2004; **279**: 5520-5527

(13) Kirito K, Watanabe T, Sawada K, Endo H, Ozawa K, Komatsu N. Thrombopoietin regulates Bcl-xL gene expression through Stat5 and phosphatidylinositol 3-kinase activation pathways. J.Biol.Chem. 2002; **277**: 8329-8337

(14) Scherr M, Chaturvedi A, Battmer K, Dallmann I, Schultheis B, Ganser A, Eder M. Enhanced sensitivity to inhibition of SHP2, STAT5, and Gab2 expression in chronic myeloid leukemia (CML). Blood 2006; **107**: 3279-3287

(15) Nyga R, Pecquet C, Harir N, Gu H, Dhennin-Duthille I, Regnier A, Gouilleux-Gruart V, Lassoued K, Gouilleux F. Activated STAT5 proteins induce activation of the PI 3-kinase/Akt and Ras/MAPK pathways via the Gab2 scaffolding adapter. Biochem.J. 2005; **390**: 359-366

(16) Lockyer HM, Tran E, Nelson BH. STAT5 is essential for Akt/p70S6 kinase activity during IL-2-induced lymphocyte proliferation. J.Immunol. 2007; **179**: 5301-5308

(17) Gu H, Pratt JC, Burakoff SJ, Neel BG. Cloning of p97/Gab2, the major SHP2-binding protein in hematopoietic cells, reveals a novel pathway for cytokine-induced gene activation. Mol.Cell 1998; **2**: 729-740

(18) Nishida K, Yoshida Y, Itoh M, Fukada T, Ohtani T, Shirogane T, Atsumi T, Takahashi-Tezuka M, Ishihara K, Hibi M, Hirano T. Gab-family adapter proteins act downstream of cytokine and growth factor receptors and T- and B-cell antigen receptors. Blood 1999; **93**: 1809-1816

(19) Crouin C, Arnaud M, Gesbert F, Camonis J, Bertoglio J. A yeast two-hybrid study of human p97/Gab2 interactions with its SH2 domain-containing binding partners. FEBS Lett. 2001; **495**: 148-153

(20) Yu WM, Hawley TS, Hawley RG, Qu CK. Role of the docking protein Gab2 in beta(1)-integrin signaling pathway- mediated hematopoietic cell adhesion and migration. Blood 2002; **99**: 2351-2359

(21) Rosa Santos SC, Dumon S, Mayeux P, Gisselbrecht S, Gouilleux F. Cooperation between STAT5 and phosphatidylinositol 3-kinase in the IL-3-dependent survival of a bone marrow derived cell line. Oncogene 2000; **19**: 1164-1172

(22) Santos SC, Lacronique V, Bouchaert I, Monni R, Bernard O, Gisselbrecht S, Gouilleux F. Constitutively active STAT5 variants induce growth and survival of hematopoietic cells through a PI 3-kinase/Akt dependent pathway. Oncogene 2001; **20**: 2080-2090

(23) Li G, Wang Z, Zhang Y, Kang Z, Haviernikova E, Cui Y, Hennighausen L, Moriggl R, Wang D, Tse W, Bunting KD. STAT5 requires the N-domain to maintain hematopoietic stem cell repopulating function and appropriate lymphoid-myeloid lineage output. Exp.Hematol. 2007; **35**: 1684-1694

(24) Zhang Y, Diaz-Flores E, Li G, Wang Z, Kang Z, Haviernikova E, Rowe S, Qu CK, Tse W, Shannon KM, Bunting KD. Abnormal hematopoiesis in Gab2 mutant mice. Blood 2007; **110**: 116-124

(25) Yilmaz OH, Valdez R, Theisen BK, Guo W, Ferguson DO, Wu H, Morrison SJ. Pten dependence distinguishes haematopoietic stem cells from leukaemia-initiating cells. Nature 2006; **441**: 475-482

(26) Hoelbl A, Kovacic B, Kerenyi MA, Simma O, Warsch W, Cui Y, Beug H, Hennighausen L, Moriggl R, Sexl V. Clarifying the role of Stat5 in lymphoid development and Abelson induced transformation. Blood 2006; **107**: 4898-4906

(27) Rocnik JL, Okabe R, Yu JC, Giese N, Schenkein DP, Gilliland DG. Roles of Tyrosine 589 and 591 in STAT5 activation and transformation mediated by FLT3-ITD. Blood 2006; **108**: 1339-1345

(28) Cain JA, Xiang Z, O'Neal J, Kreisel F, Colson A, Luo H, Hennighausen L, Tomasson MH. Myeloproliferative disease induced by TEL-PDGFRB displays dynamic range sensitivity to Stat5 gene dosage. Blood 2007; **109**: 3906-3914

(29) Bumm TG, Elsea C, Corbin AS, Loriaux M, Sherbenou D, Wood L, Deininger J, Silver RT, Druker BJ, Deininger MW. Characterization of murine JAK2V617F-positive myeloproliferative disease. Cancer Res. 2006; **66**: 11156-11165

(30) Huang J, Manning BD. A complex interplay between Akt, TSC2 and the two mTOR complexes. Biochem.Soc.Trans. 2009; **37**: 217-222

(31) Mohi MG, Boulton C, Gu TL, Sternberg DW, Neuberg D, Griffin JD, Gilliland DG, Neel BG. Combination of rapamycin and protein tyrosine kinase (PTK) inhibitors for the treatment of leukemias caused by oncogenic PTKs. Proc.Natl.Acad.Sci.U.S.A 2004; **101**: 3130-3135

(32) Corbacioglu S, Kilic M, Westhoff MA, Reinhardt D, Fulda S, Debatin KM. Newly identified c-KIT receptor tyrosine kinase ITD in childhood AML induces ligand-independent growth and is responsive to a synergistic effect of imatinib and rapamycin. Blood 2006; **108**: 3504-3513

(33) Wei G, Twomey D, Lamb J, Schlis K, Agarwal J, Stam RW, Opferman JT, Sallan SE, den Boer ML, Pieters R, Golub TR, Armstrong SA. Gene expression-based chemical genomics identifies rapamycin as a modulator of MCL1 and glucocorticoid resistance. Cancer Cell 2006; **10**: 331-342

(34) Kim KW, Moretti L, Mitchell LR, Jung DK, Lu B. Combined Bcl-2/mammalian target of rapamycin inhibition leads to enhanced radiosensitization via induction of apoptosis and autophagy in non-small cell lung tumor xenograft model. Clin.Cancer Res. 2009; **15**: 6096-6105

(35) Ackler S, Xiao Y, Mitten MJ, Foster K, Oleksijew A, Refici M, Schlessinger S, Wang B, Chemburkar SR, Bauch J, Tse C, Frost DJ, Fesik SW, Rosenberg SH, Elmore SW, Shoemaker AR. ABT-263 and rapamycin act cooperatively to kill lymphoma cells in vitro and in vivo. Mol.Cancer Ther. 2008; **7**: 3265-3274

(36) Tse C, Shoemaker AR, Adickes J, Anderson MG, Chen J, Jin S, Johnson EF, Marsh KC, Mitten MJ, Nimmer P, Roberts L, Tahir SK, Xiao Y, Yang X, Zhang H, Fesik S, Rosenberg SH, Elmore SW. ABT-263: a potent and orally bioavailable Bcl-2 family inhibitor. Cancer Res. 2008; **68**: 3421-3428

(37) Yoshimoto G, Miyamoto T, Jabbarzadeh-Tabrizi S, Iino T, Rocnik JL, Kikushige Y, Mori Y, Shima T, Iwasaki H, Takenaka K, Nagafuji K, Mizuno S, Niiro H, Gilliland GD, Akashi K. FLT3-ITD up-regulates MCL-1 to promote survival of stem cells in acute myeloid leukemia via FLT3-ITD-specific STAT5 activation. Blood 2009; **114**: 5034-5043

(38) Tahir SK, Wass J, Joseph MK, Devanarayan V, Hessler P, Zhang H, Elmore SW, Kroeger PE, Tse C, Rosenberg SH, Anderson MG. Identification of Expression Signatures Predictive of Sensitivity to the Bcl-2 Family Member Inhibitor ABT-263 in Small Cell Lung Carcinoma and Leukemia/Lymphoma Cell Lines. Mol.Cancer Ther. 2010

(39) Janes MR, Limon JJ, So L, Chen J, Lim RJ, Chavez MA, Vu C, Lilly MB, Mallya S, Ong ST, Konopleva M, Martin MB, Ren P, Liu Y, Rommel C, Fruman DA. Effective and selective targeting of leukemia cells using a TORC1/2 kinase inhibitor. Nat.Med. 2010; **16**: 205-213

**Titles and legends to figures:**

**Figure 1. Deletion of Gab2 attenuates myeloid hyperplasia and improves survival of mice expressing persistently active STAT5.** Wild-type or Gab2$^{-/-}$ mouse BM cells were retrovirally-transduced with either IR-GFP control vector (IR) or STAT5a$^{S711F}$, and transplanted into lethally irradiated recipients on 3 separate experiments. Mice were analyzed at the same time for all groups (26-32 days after transplant). **A.** Total WBC counts are plotted for mice of various genotypes. Each dot represents an individual mouse that was analyzed. **B.** The absolute number of Gr-1/Mac-1 double positive cells in mice of

various genotypes. Horizontal bars indicate the average for all mice analyzed per group. **C.** The spleen weights were measured and plotted against each genotype analyzed. **D.** The Kaplan-Meier survival curve of mice expressing persistently active STAT5a or IR-GFP control vector was also determined by following mice daily and recording deaths. The number of mice per group was as follows: WT-IR N=6; Gab2$^{-/-}$ IR N=6; Gab2$^{-/-}$ STAT5a$^{S711F}$ N=6; WT STAT5a$^{S711F}$ N=7. IR denotes IR-GFP vector and STAT5a$^{S711F}$ denotes STAT5a$^{S711F}$-IR-GFP vector. The P value in panel D (log-rank test) represents the comparison of survival by STAT5a$^{S711F}$ on wild-type vs. Gab2$^{-/-}$ background.

**Figure 2. Deletion of Gab2 attenuates liver and spleen pathology resulting from expression of persistently active STAT5.** Tissues from transplanted mice expressing either STAT5a$^{S711F}$ or IR-GFP control vector were collected, formalin fixed, and histologic sections were stained with hematoxylin and eosin (H&E). Representative sections of liver and spleen are shown. The liver **(A)** or spleen **(C)**, at 20X magnification was analyzed for wild-type and Gab2$^{-/-}$ BM transplanted mice expressing the IR-GFP control vector. The liver **(B)** or spleen **(D)** was also analyzed at 20X and 40X magnification for wild-type and Gab2$^{-/-}$ groups expressing STAT5a$^{S711F}$.

**Figure 3. Inhibition of myeloid colony-formation resulting from STAT5a$^{S711F}$ or MPL$^{W506L}$ expression by treatment with rapamycin. A.** Wild-type BM cells were retrovirally-transduced with MSCV-STAT5a$^{S711F}$-IR-GFP, sorted for GFP$^{+}$ cells, and plated in methylcellulose medium. The average number of colonies (from duplicate plating) was determined in the absence or presence of recombinant IL-3 (20 ng/ml), IL-6 (50 ng/ml), and SCF (50 ng/ml) from three independent assays that yielded comparable results. **B.** Wild-type BM cells were retrovirally-transduced with MSCV-MPL$^{W506L}$-IR-YFP, sorted for YFP$^{+}$ cells, and plated in the presence or absence of 2 ng/ml recombinant IL-3.

**Figure 4. Rapamycin inhibits myeloid expansion in the peripheral blood and prolongs the survival of mice expressing STAT5a$^{S711F}$.**

BM cells were transduced with retroviral vectors expressing either IR-GFP or STAT5a$^{S711F}$. Equal donor equivalents of GFP$^{+}$ cells were subsequently transplanted into irradiated recipients. One month post transplantation, mice were treated with either rapamycin (4 mg/kg every other day) or vehicle control by i.p. injection for 3-4 weeks and then discontinued. Peripheral white blood cell counts were determined at the indicated times after treatment. IR-GFP control mice treated with either vehicle control (**A**), or rapamycin (**B**), and STAT5a$^{S711F}$ expressing mice treated with either vehicle (**C**), or rapamycin (**D**). Each line represents an individual mouse. **E.** The 4 groups of mice were monitored daily and mouse deaths were recorded. Mouse survival was plotted on Kaplan-Meier curve. IR-GFP vehicle control, N=3; IR-GFP rapamycin, N=3; STAT5a$^{S711F}$ vehicle control, N=9; STAT5a$^{S711F}$ rapamycin, N=10. The P value in panel E (log-rank test) represents the comparison of survival in mice expressing STAT5a$^{S711F}$ treated with rapamycin vs. vehicle control.

**Figure 5. Rapamycin combined with ABT-737 synergistically kills transduced BaF3 cells expressing STAT5a$^{S711F}$, BCR-ABL, or TEL-JAK2. A.** BaF3 cells were transduced with the IR-GFP, STAT5a$^{S711F}$, BCR-ABL, or TEL-JAK2 vector. The cells were treated with 1 nM rapamycin overnight. Recombinant IL-3 at a minimal concentration of 0.01 ng/ml was added to IR-GFP cells to maintain their viability. Cell extracts were resolved by SDS-PAGE and immunoblot was performed with the indicated antibody. **B.** Cells were cultured in serial concentrations of rapamycin for 48 hours and cell expansion was measured by manual scoring using a hemacytometer. **C.** Cells were cultured with the indicated concentration of ABT-737 for 48 hours and cell viability was measured by trypan blue exclusion. **D.** Cells were cultured in 0.2 ng/ml IL3 or without IL3 as indicated. For each group, the cells were treated with either rapamycin (1nM) or ABT-737 (5μm) alone or combination. After 48 hours, cell death was determined by trypan blue exclusion assay. P values shown are for comparison of ABT-737 alone vs. ABT-737/Rapamycin combination groups.

**Figure 6. Rapamycin combined with ABT-737 synergistically kills human K562 cells.** **(A, E)** K562 cells and NB4 cells were cultured at the indicated concentration of rapamycin overnight. The rapamycin activity was determined by phosphorylation of the p70S6K protein. Total p70S6K was used a control. **(B, F)** K562 and NB4 cells were cultured in the indicated concentration of rapamycin for 48 hours and the fold proliferation of the cells was determined by manual cell count. **(C, G)** K562 cells and NB4 cells were cultured in the presence of ABT-737 for 48 hours. The cell viability were determined by both PI staining and trypan blue exclusion. Both methods gave similar results. **(D, H)** K562 and NB4 cells were cultured in either rapamycin alone (10 nM), ABT-737 alone (5μM), or the combination of both for 48 hours. Cell viability was determined as described in Methods.

**Figure 7. Proposed model for targeting synergistic signaling nodes mediated by distinct STAT5 survival targets in myeloproliferative disease.** Based on our earlier studies, it was important to assess the impact of the Gab2 interaction and PI3K/Akt pathway activation in the pathophysiology of MPD induced by persistently activated STAT5. In the STAT5a$^{S711F}$ murine retroviral transduction model we were able to initiate MPD at the level of STAT5 without activating first the upstream receptor or non-receptor tyrosine kinases which would simultaneously activate PI3K/Akt at the receptor level. Using genetic deletion of Gab2 or pharmacologic inhibition of mTOR with rapamycin, we were able to interrogate this signaling axis and determine its importance in the development and progression of MPD. Note that this diagram is overly simplified regarding PLCγ and MAPK pathway activation in order to focus on STAT5 and PI3K/Akt activation.

Type of file: figure
Label: 1
Filename: figure_1.tif

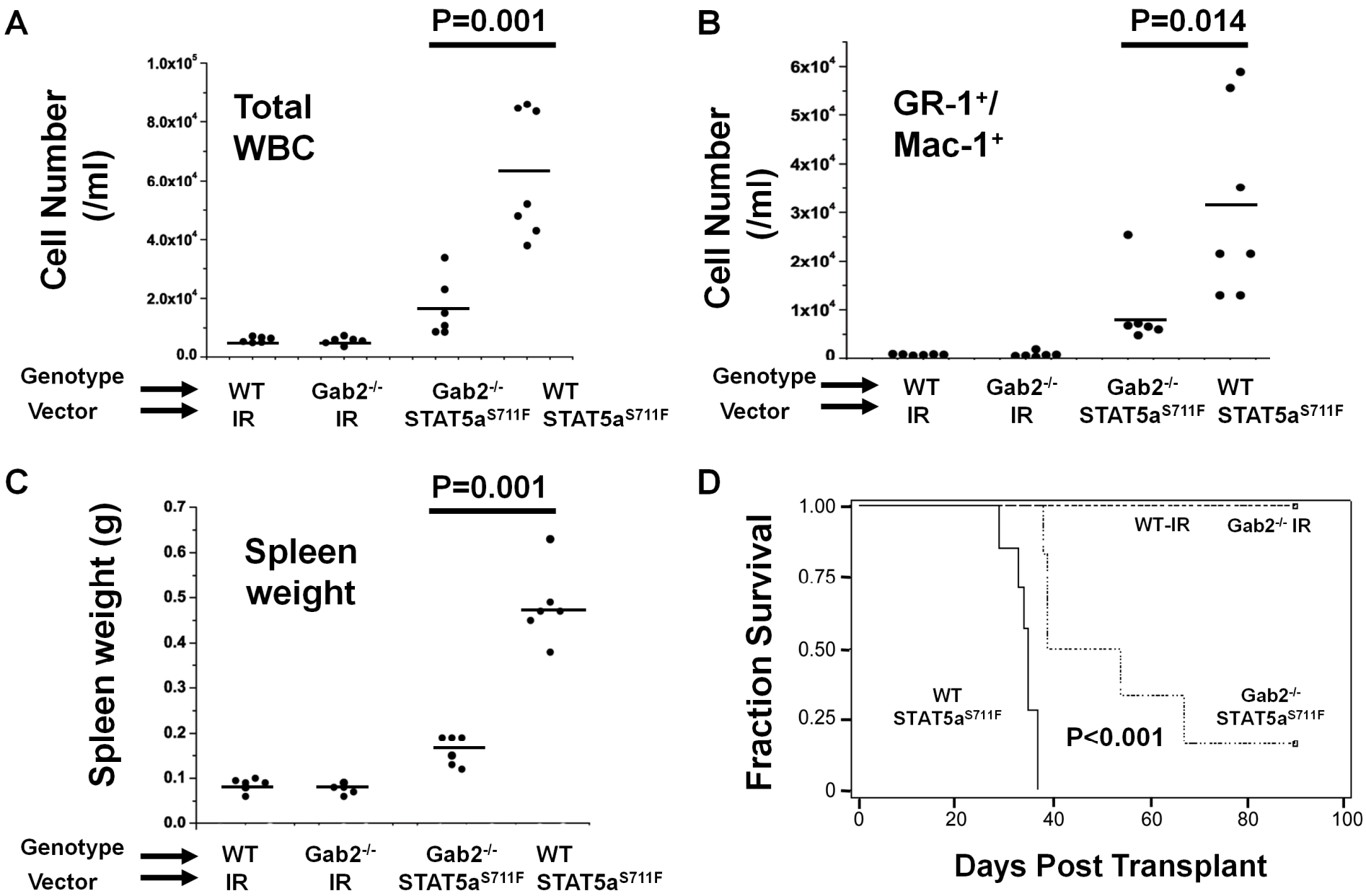
A
P=0.001
Total WBC
Cell Number (/ml)
1.0x10^5
8.0x10^4
6.0x10^4
4.0x10^4
2.0x10^4
0.0
Genotype
Vector
WT IR
Gab2-/- IR
Gab2-/- STAT5aS711F
WT STAT5aS711F
B
P=0.014
GR-1+/ Mac-1+
Cell Number (/ml)
6x10^4
5x10^4
4x10^4
3x10^4
2x10^4
1x10^4
0
Genotype
Vector
WT IR
Gab2-/- IR
Gab2-/- STAT5aS711F
WT STAT5aS711F
C
P=0.001
Spleen weight
Spleen weight (g)
0.7
0.6
0.5
0.4
0.3
0.2
0.1
0.0
Genotype
Vector
WT IR
Gab2-/- IR
Gab2-/- STAT5aS711F
WT STAT5aS711F
D
Fraction Survival
1.00
0.75
0.50
0.25
0
WT-IR
Gab2-/- IR
WT STAT5aS711F
Gab2-/- STAT5aS711F
P<0.001
0
20
40
60
80
100
Days Post Transplant

Figure 1

Type of file: figure
Label: 2
Filename: figure_2.tif

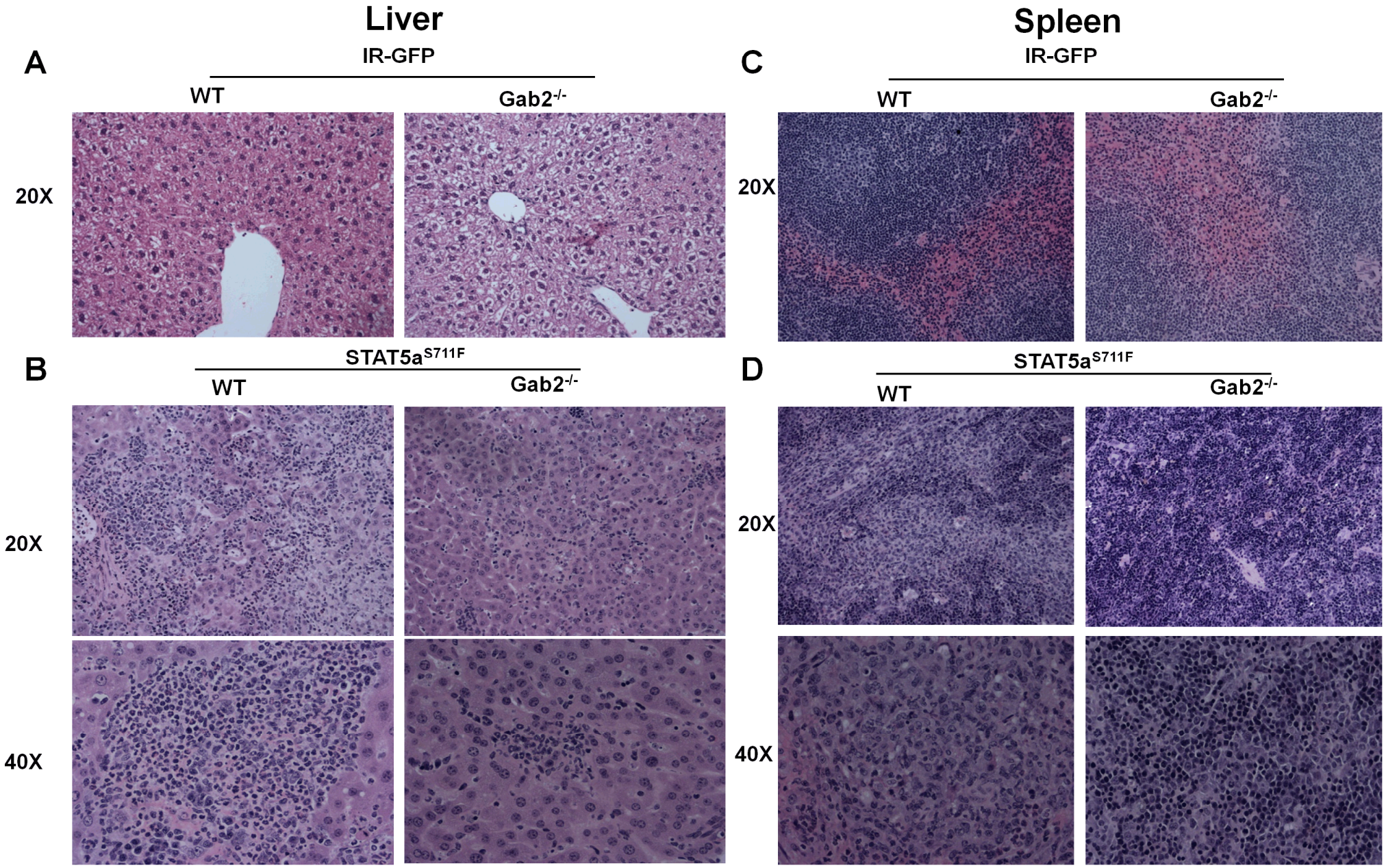
Liver
Spleen
A
IR-GFP
WT
Gab2-/-
20X
B
STAT5aS711F
WT
Gab2-/-
20X
40X
C
IR-GFP
WT
Gab2-/-
20X
D
STAT5aS711F
WT
Gab2-/-
20X
40X

Figure 2

Type of file: figure
Label: 3
Filename: figure_3.tif

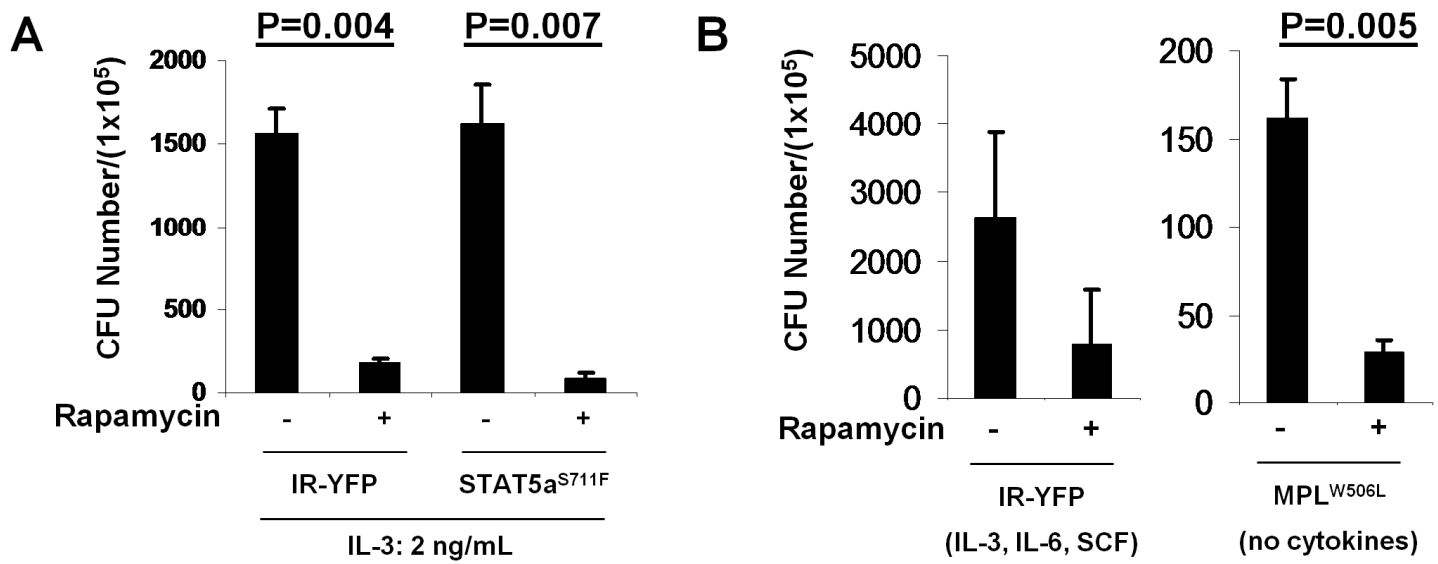
A
P=0.004
P=0.007
CFU Number/(1x10^5)
2000
1500
1000
500
0
Rapamycin
-
+
-
+
IR-YFP
STAT5a^S711F
IL-3: 2 ng/mL
B
P=0.005
CFU Number/(1x10^5)
5000
4000
3000
2000
1000
0
200
150
100
50
0
Rapamycin
-
+
-
+
IR-YFP
(IL-3, IL-6, SCF)
MPL^W506L
(no cytokines)

Figure 3

Type of file: figure
Label: 4
Filename: figure_4.tif

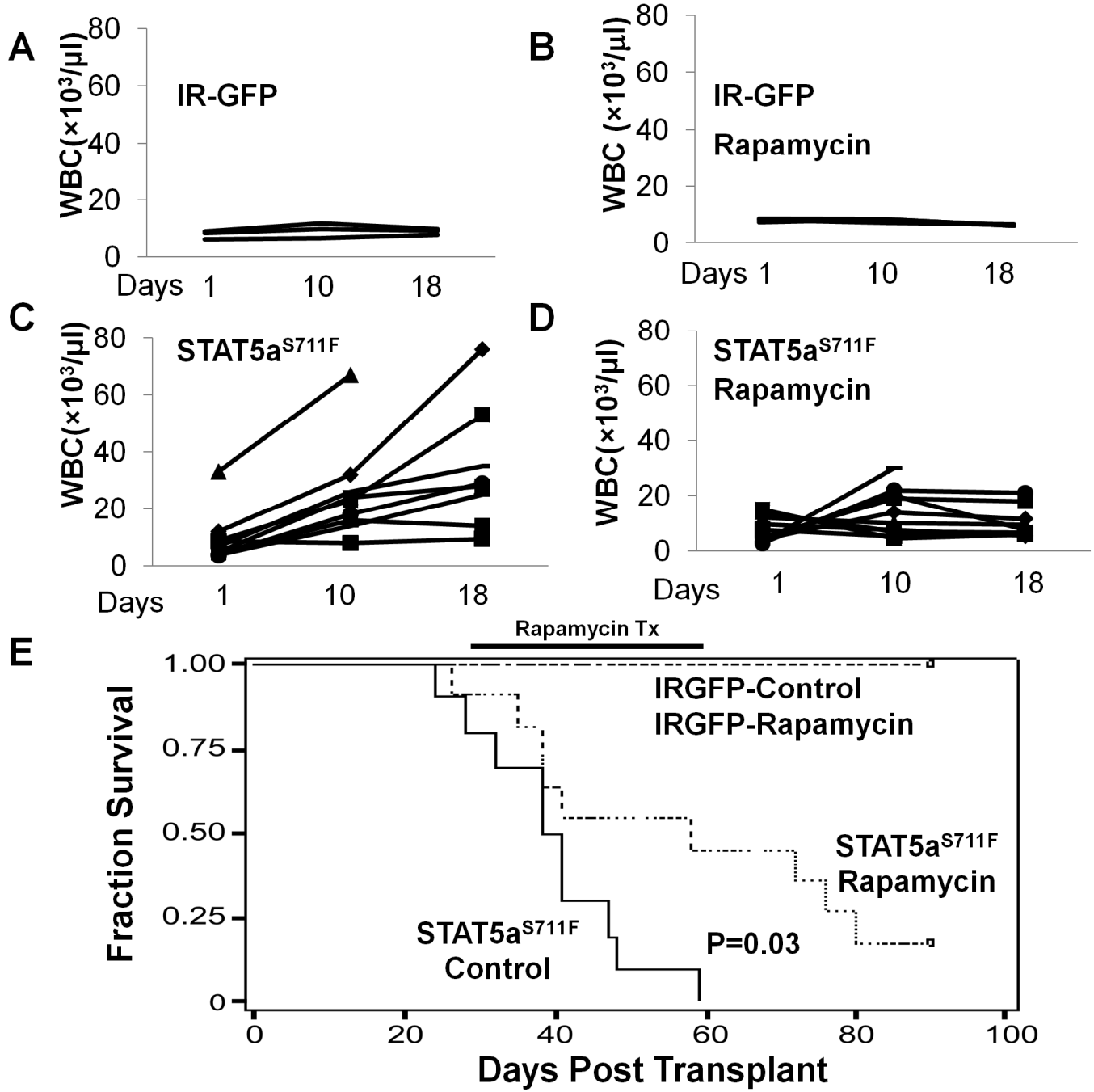
A
IR-GFP
WBC(×10³/µl)
80
60
40
20
0
Days 1 10 18
B
IR-GFP
Rapamycin
WBC (×10³/µl)
80
60
40
20
0
Days 1 10 18
C
STAT5a$^{S711F}$
WBC(×10³/µl)
80
60
40
20
0
Days 1 10 18
D
STAT5a$^{S711F}$
Rapamycin
WBC(×10³/µl)
80
60
40
20
0
Days 1 10 18
E
Rapamycin Tx
Fraction Survival
1.00
0.75
0.50
0.25
0
IRGFP-Control
IRGFP-Rapamycin
STAT5a$^{S711F}$
Rapamycin
STAT5a$^{S711F}$
Control
P=0.03
0 20 40 60 80 100
Days Post Transplant

Figure 4

Type of file: figure
Label: 5
Filename: figure_5.tif

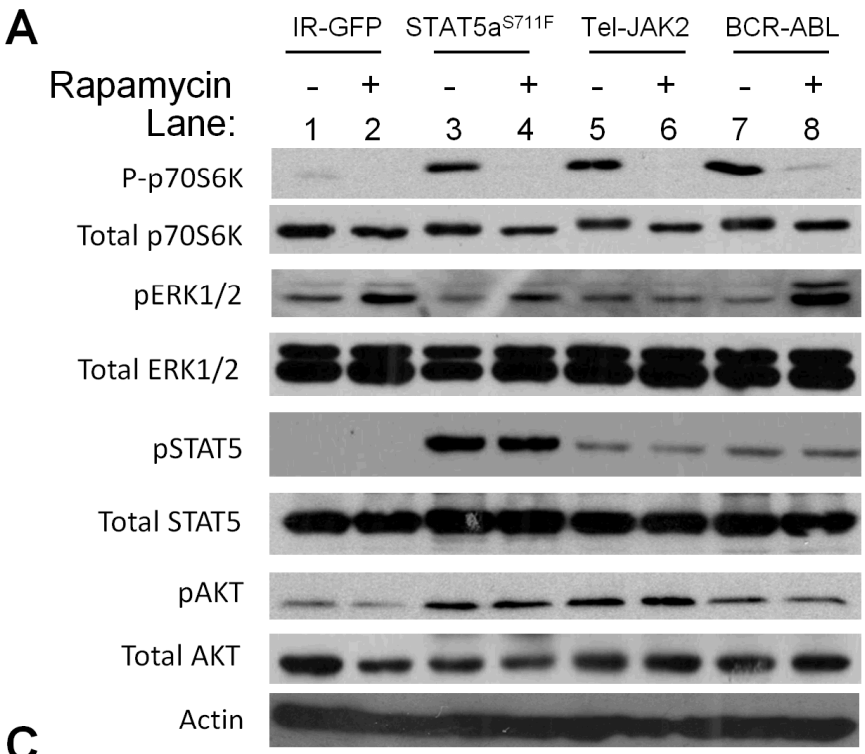
A
IR-GFP
STAT5a$^{S711F}$
Tel-JAK2
BCR-ABL
Rapamycin
- + - + - + - +
Lane:
1 2 3 4 5 6 7 8
P-p70S6K
Total p70S6K
pERK1/2
Total ERK1/2
pSTAT5
Total STAT5
pAKT
Total AKT
Actin

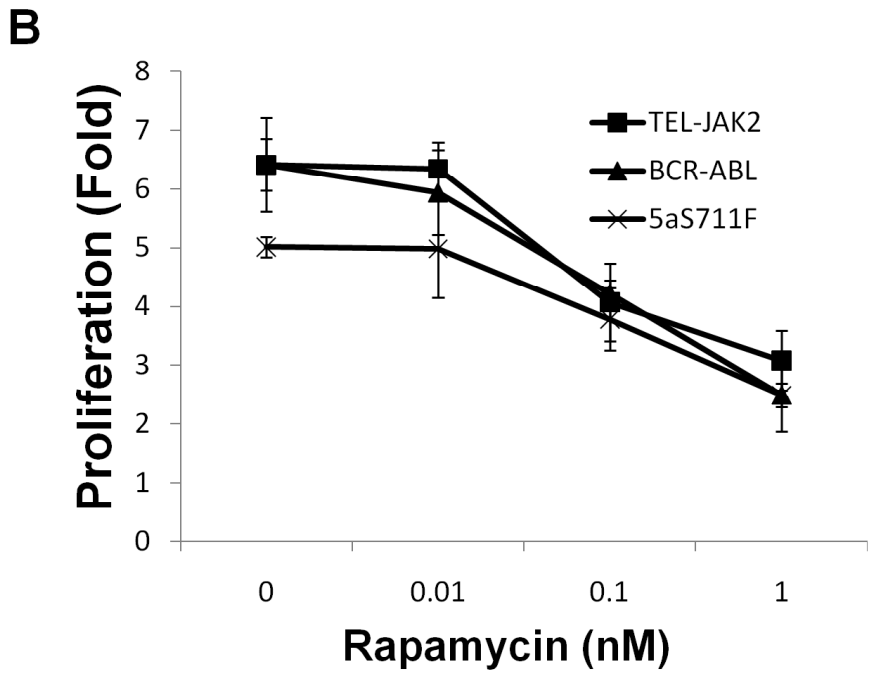
B
Proliferation (Fold)
0
1
2
3
4
5
6
7
8
TEL-JAK2
BCR-ABL
5aS711F
0
0.01
0.1
1
Rapamycin (nM)

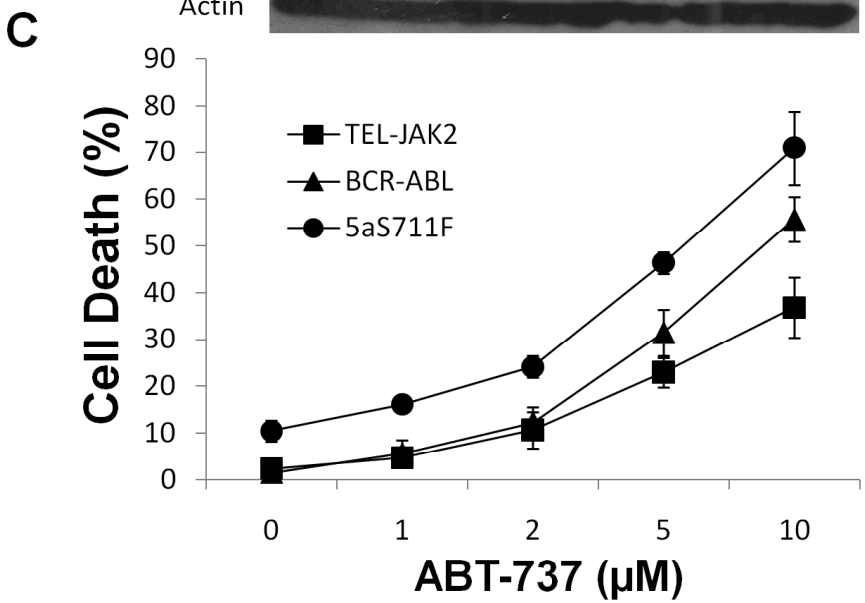
C
Cell Death (%)
0
10
20
30
40
50
60
70
80
90
TEL-JAK2
BCR-ABL
5aS711F
0
1
2
5
10
ABT-737 (μM)

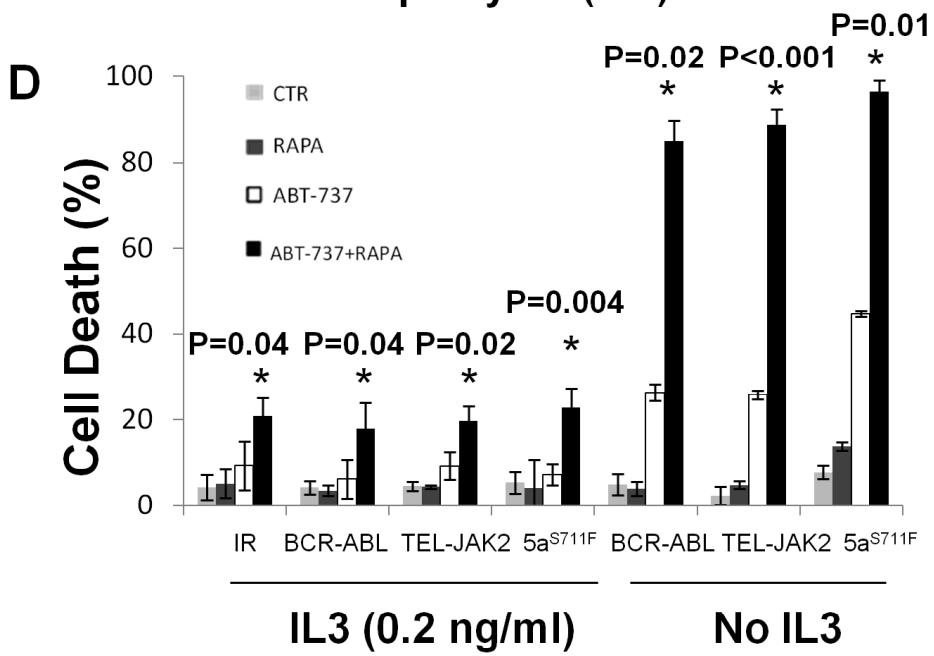
D
Cell Death (%)
0
20
40
60
80
100
CTR
RAPA
ABT-737
ABT-737+RAPA
P=0.04
P=0.04
P=0.02
P=0.004
P=0.02
P<0.001
P=0.01
IR
BCR-ABL
TEL-JAK2
5a$^{S711F}$
BCR-ABL
TEL-JAK2
5a$^{S711F}$
IL3 (0.2 ng/ml)
No IL3

Figure 5

Type of file: figure
Label: 6
Filename: figure_6.tif

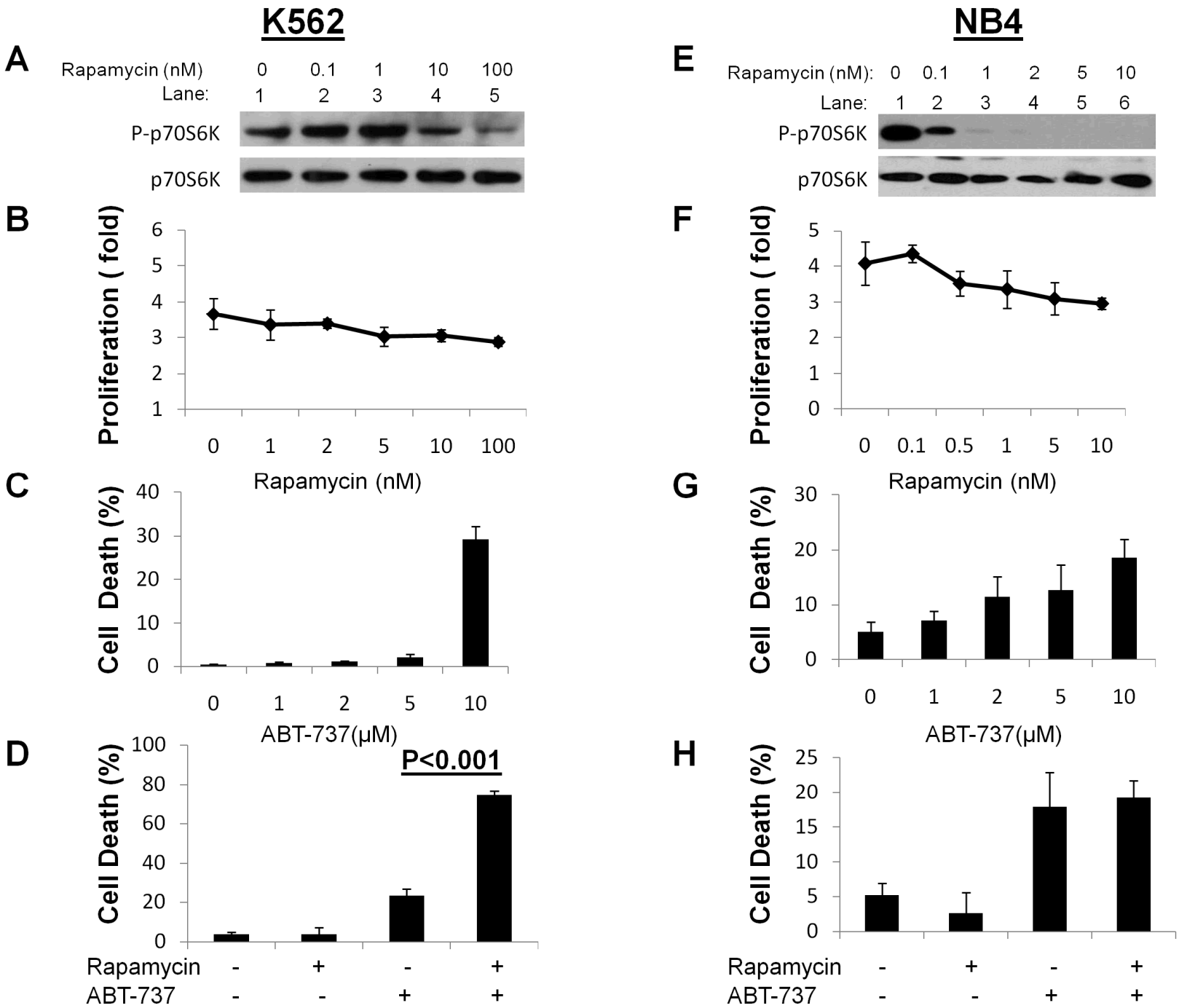
K562
NB4
A
Rapamycin (nM) 0 0.1 1 10 100
Lane: 1 2 3 4 5
P-p70S6K
p70S6K
E
Rapamycin (nM): 0 0.1 1 2 5 10
Lane: 1 2 3 4 5 6
P-p70S6K
p70S6K
B
Proliferation ( fold)
Rapamycin (nM)
F
Proliferation ( fold)
Rapamycin (nM)
C
Cell Death (%)
ABT-737(μM)
G
Cell Death (%)
ABT-737(μM)
D
Cell Death (%)
P<0.001
Rapamycin - + - +
ABT-737 - - + +
H
Cell Death (%)
Rapamycin - + - +
ABT-737 - - + +

Figure 6

Type of file: figure
Label: 7
Filename: figure_7.tif

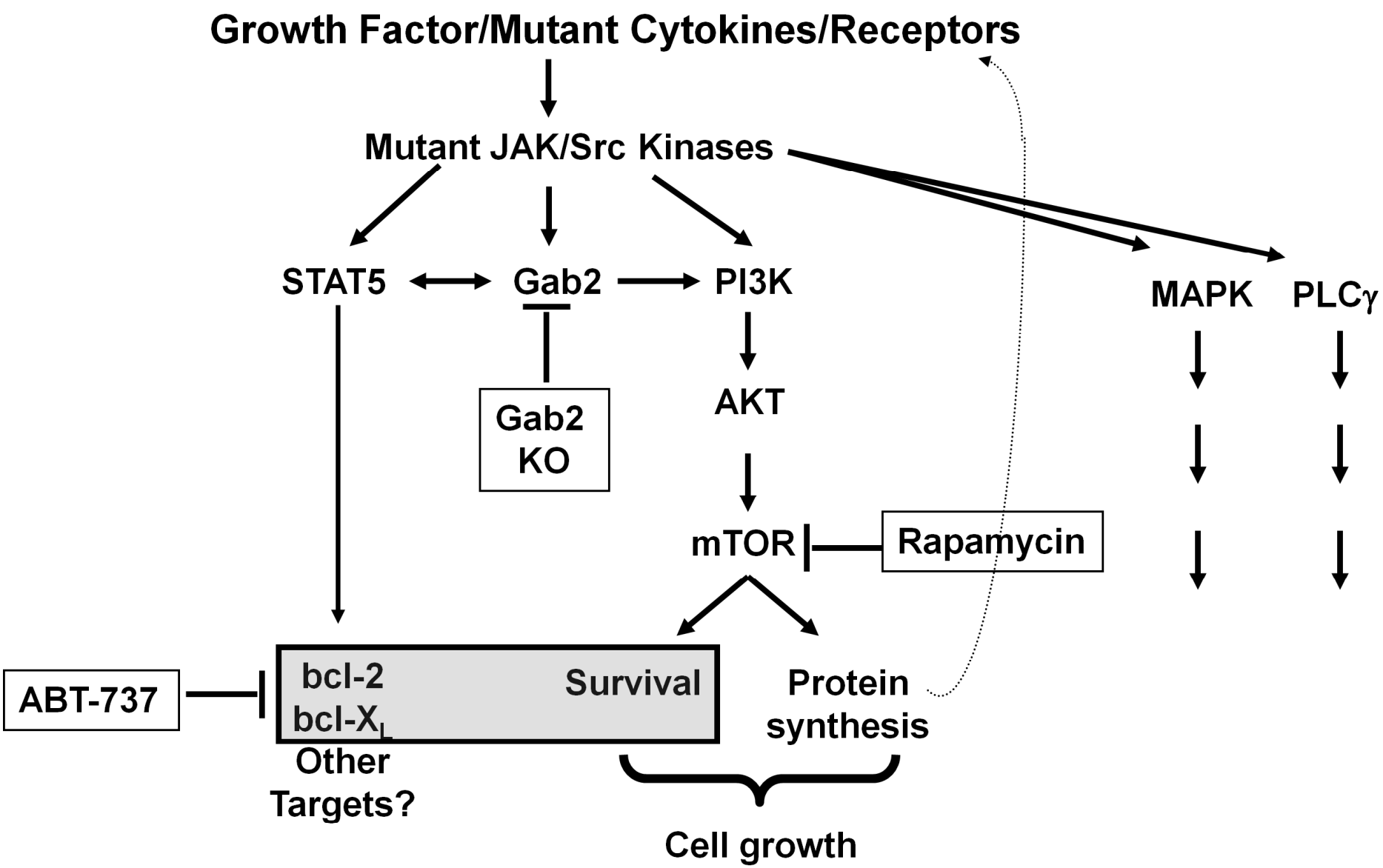
Growth Factor/Mutant Cytokines/Receptors
Mutant JAK/Src Kinases
STAT5
Gab2
PI3K
MAPK
PLCγ
Gab2 KO
AKT
mTOR
Rapamycin
ABT-737
bcl-2
bcl-XL
Survival
Other Targets?
Protein synthesis
Cell growth

Figure 7

The NIHMS has received the file 'supp_info_1.doc' as supplementary data. The file will not appear in this PDF Receipt, but it will be linked to the web version of your manuscript.

The NIHMS has received the file 'supp_info_2.tif' as supplementary data. The file will not appear in this PDF Receipt, but it will be linked to the web version of your manuscript.

The NIHMS has received the file 'supp_info_3.tif' as supplementary data. The file will not appear in this PDF Receipt, but it will be linked to the web version of your manuscript.

The NIHMS has received the file 'supp_info_4.tif' as supplementary data. The file will not appear in this PDF Receipt, but it will be linked to the web version of your manuscript.

The NIHMS has received the file 'supp_info_5.tif' as supplementary data. The file will not appear in this PDF Receipt, but it will be linked to the web version of your manuscript.